# Expression of p190A during Apoptosis in the Regressing Rat Ventral Prostate*

COLM MORRISSEY, STEFFANY BENNETT, ESTHER NITSCHE,
R. SEAN GUENETTE, PAUL WONG, AND MARTIN TENNISWOOD

*Department of Biological Sciences, University of Notre Dame (C.M., S.B., R.S.G., M.T.), Notre Dame, Indiana 46556; the Cell and Molecular Biology Graduate Program, University College Dublin (C.M.), Dublin 4, Ireland; the Institute of Neuroscience, Carleton University (S.B.), Ottawa, Ontario, Canada K1S 5B6; the Department of Pediatrics, University of Lubeck (E.N.), D-23538 Lubeck, Germany; and the Department of Biological Sciences, University of Alberta (P.W.), Edmonton, Alberta, Canada T6G2E9*

**ABSTRACT**

After hormonal ablation, 90% of the secretory epithelial cells of the prostate undergo apoptosis, and the remaining cells are reorganized as the tissue is remodeled. Using differential display RT-PCR of total RNA extracted from the rat ventral prostate before and 4 days after castration, we have cloned and sequenced a number of complementary DNAs whose cognate messenger RNAs (mRNAs) may be either up- or down-regulated during prostatic regression. One sequence of particular interest, 25.2, is up-regulated after castration and is homologous to p190, a protein associated with cytoskeletal reorganization. RT-PCR has confirmed that the steady state level of p190A mRNA is increased in the rat ventral prostate after castration, and Western blot analysis indicates that the protein levels for p190A also increase. The steady state level of p190B mRNA, the second isoform

of p190, does not appear to change significantly after hormone ablation. Immunohistochemical analysis demonstrates that p190A is up-regulated primarily in the columnar epithelial cells that actively undergo cell death after hormone ablation. As Rho-GAP signaling had been shown to be influenced by p190 levels, leading to the disassembly of focal adhesion contacts and the loss of cytoskeletal architecture, we also measured the changes in Rho-GAP during prostate regression. Rho-GAP levels do not change significantly, suggesting that changes in stoichiometry of the interaction between p190A and Rho-GAP may be a prerequisite for the initiation of cytoplasmic condensation. These intracellular events coupled with the proteolytic degradation of the extracellular matrix appear to be integral to the apoptotic process in glandular epithelia. (*Endocrinology* **140:** 3328–3333, 1999)

CELL DEATH, or apoptosis, is not a single phenomenon, but, rather, a series of morphologically and biochemically related processes (1–3). Cell death of lymphocytes and other cells of reticulo-endothelial origin is dominated by changes in nuclear morphology (4) and mitochondrial biology (5, 6), whereas apoptotic death of glandular epithelial cells, such as those of the prostate, also requires profound cytoplasmic changes and alterations in the cell-cell and cell-substratum interactions (7). The rodent prostate is a useful model for the study of apoptosis induced by hormone withdrawal, as the secretory epithelial cells are localized in the distal and intermediate regions of the ducts (8–10) and are critically dependent on androgens for survival (11). Changes in the expression of a number of genes, including clusterin (8, 10, 12, 13), and a number of extracellular proteases, including cathepsin B (14), cathepsin D (15), and plasminogen activators (16), have been shown to be induced during regression of the gland. The expression and activation of these proteases appear to result in the degradation of specific components of the extracellular matrix (ECM), including fibronectin, collagen, laminin, and vitronectin (13, 17). These components of the ECM interact with their cognate receptors,

most of which are members of the integrin superfamily (18). The integrins are localized on the basal surface of epithelial cells and ensure that the cells have the structural underpinnings required for polarization, vectorial transport, and secretion (19, 20). The ECM components and their respective membrane receptors are expressed in hormone-replete animals, and their synthesis is under tight regulation to ensure that the glandular morphology and differentiated, secretory phenotype are maintained (17, 21–23).

We have recently used differential display RT-PCR to identify additional genes that may be induced during apoptosis in the regressing prostate. We report here that one sequence of particular interest, 25.2, has homology to p190 messenger RNA (mRNA). To date, two related p190 proteins have been identified. These proteins are GAP [guanosine triphosphatase (GTPase)-activating protein]-associated proteins that have been implicated in the regulation of the cytoskeleton and focal contacts through the interaction with the p120 Ras-GAP and Rho family of small guanine nucleotide-binding proteins (24). The demonstration that a component of the intracellular signaling network regulating focal adhesion kinase is up-regulated during apoptotic cell death suggests that cell-substratum interactions may be disrupted by proteolysis and/or by inside-out signaling.

## Materials and Methods

### Animals

Male Sprague Dawley rats (250–300 g) were obtained from Taconic Farms, Inc. (Germantown, NY). Animals were maintained in a con-

trolled environment (12 h of light, 12 h of darkness) and received Purina rodent chow (Ralston Purina Co., St. Louis, MO) and water *ad libitum*. The animals were castrated via the scrotal route under light halothane anesthesia. Animals were killed by cervical dislocation on different days after castration, and the prostate glands were excised and processed immediately or stored in liquid nitrogen.

### Differential display

Total RNA was isolated from Sprague Dawley rat ventral prostates before and 4 days after castration using RNAzol B (Biotex Laboratories, Inc., Houston, TX). Twenty-five milligrams of total RNA were deoxyribonuclease (DNase) treated with 5 U [ribonuclease (RNase) free] DNase (Promega Corp., Madison, WI), $1 \times$ DNase buffer, and 10 U RNAsin at 37 C for 30 min and reverse transcribed using the RNAmap protocol (GenHunter Corp., Brookline, MA) with Superscript II RNase H- (Life Technologies, Grand Island, NY) and the downstream primer $T_{12}MC$ (GenHunter Corp.). The reverse transcribed product was amplified by PCR using AP-5 (GTTGCGATCC) and $T_{12}MC$ primers and 2.5 U AmpliTaq (Perkin Elmer, Branchburg, NJ) in the presence of $[\alpha^{-35}S]$deoxy-ATP (1000 Ci/mmol; Amersham, Arlington Heights, IL) The PCR conditions were as follows: 30 sec at 94 C, 2 min at 40 C, and 30 sec at 72 C for 40 cycles. The reaction products were electrophoresed on 6% denaturing polyacrylamide gels at 1500 V for 2 h, dried for 1 h at 80 C, and exposed to x-ray film (Fuji Photo Film Co., Ltd., Tokyo, Japan) at $-80$ C with an intensifying screen for 48 h. Bands of interest were cut from the gel, boiled, filtered through ultrafree MC 0.45-$\mu$m filters (Millipore Corp., Bedford, MA), ethanol precipitated, and redissolved in $H_2O$. The products were reamplified by PCR using the AP-5 and $T_{12}MC$ primers and the same reaction conditions as the differential display, cloned into the pCRII vector (Invitrogen, San Diego, CA), and sequenced.

### RNase protection assays

The pCRII vector containing the gene fragment 25.2 was linearized with *Bam*HI and transcribed according to the manufacturer's guidelines using the MAXIscript *in vitro* transcription kit (Ambion, Inc., Austin, TX) to produce a 226-bp $[\alpha^{-32}P]$UTP (3000 Ci/mmol) (Amersham)-labeled antisense probe. The 226-bp antisense probe was hybridized with 10 $\mu$g total RNA isolated from rat ventral prostate from days 0, 2, and 4 after castration and RNase digested using the RPA II kit (Ambion, Inc.). The products were electrophoresed on 5% 7 M urea polyacrylamide gels at 200 V for 2 h. The gels were dried down at 80 C for 1 h and exposed to X-Omat AR film (Eastman Kodak Co., Rochester, NY) at $-80$ C with an intensifying screen for 24 h.

### Northern analysis

A multiple tissue Northern blot of rat tissues (CLONTECH Laboratories, Inc., Palo Alto, CA) was prehybridized for 2 h in 10% dextran sulfate, 1% SDS, $6 \times$ SSC ($1 \times$ SSC is 150 mM NaCl and 15 mM sodium citrate, pH 7.0), 1% sheared salmon sperm DNA, and $5 \times$ Denhart's solution ($100 \times$ Denhart's solution is 2% BSA, 2% polyvinyl pyrrolidone, and 2% Ficoll) and hybridized with radiolabeled 25.2 ($2 \times 10^6$ cpm/ml) for 24 h at 63 C in a hybridization oven. After hybridization, the membrane was washed once at 63 C in $2 \times$ SSC for 15 min, once in $2 \times$ SSC-0.1% SDS for 30 min, and once in $0.1 \times$ SSC-0.1% SDS for 10 min and exposed to X-Omat AR film (Eastman Kodak Co.) at $-80$ C for 16 days.

### RT-PCR

Polyadenylated mRNA, prepared by oligo(deoxythymidine)-cellulose chromatography (25), was reverse transcribed from rat ventral prostate on days 0, 2, and 4 after castration. p190A and glyceraldehyde-3-phosphate dehydrogenase (GAPDH) were amplified in a reaction mix containing 60 mM Tris-HCl, 15 mM $(NH_4)SO_4$, and 2 mM $MgCl_2$, pH 9.5; 1 mM deoxy-NTPs; 0.5 pmol p190A reverse primer (tgcgtccataaccaatgcca); and 0.5 pmol p190A forward primer (gcccgagagttagccaatgaaa). After 2 min at 94 C, 3 U *Taq* polymerase (Life Technologies) were added, and PCR was continued for 30 cycles of 1 min at 60 C, 1 min at 72 C, and 30 sec at 94 C and a final cycle of 10 min at 72 C. After the first 6 cycles, 0.5 pmol GAPDH forward primer (cctctctcttgctctcagtat) and 0.5 pmol

GAPDH reverse primer (gtatccgttgtggatctgaca) were added to the reaction mix. Amplification of p190B and GAPDH used the same reaction conditions, except the reaction was for 25 cycles, and the p190B primers were 0.5 pmol p190B reverse primer (cagtaactgccaccagctgt) and 0.5 pmol p190B forward primer (gccatgtgtggagatccatt). The primers were designed using Primers3 Software (http://www.genome.wi.mit.edu/cgi-bin/primer/primer3.cgi), based on the available sequences for rat p190A and human p190B. The gels were photographed using UV transillumination (306 nm), and the photographs were scanned using a ScanJet Plus scanner and HP Scanning Gallery Plus 5.0 software (Hewlett-Packard Co., Palo Alto, CA). The scanned images were quantitated using SigmaGel (Jandel Scientific Software, San Rafael, CA). The data were graphed using GraphPad Prism 1.0 (GraphPad Software, Inc., San Diego, CA).

### Immunohistochemistry

Frozen sections (10 $\mu$m) of ventral prostates, excised at various times after castration, were prepared on gelatin-coated slides, fixed in 4% paraformaldehyde for 20 min, and washed three times in 10 mM PBS. The sections were incubated with the appropriate dilution (1:300) of the primary antibody, anti-p190 Rho-GAP (Transduction Laboratories, Inc., Lexington, KY), which is specific for p190A (24), at 4 C overnight, washed three times in 10 mM PBS, incubated with goat antimouse fluorescein isothiocyanate secondary antibody (1:100; Sigma Chemical Co., St. Louis, MO) at 37 C for 30 min, washed three times in 10 mM PBS, and coverslipped with mounting medium (Vector Laboratories, Inc., Burlingame, CA). Sections were examined and photographed under indirect fluorescence using a Nikon Optiphot-2 microscope (Nikon, Melville, NY). Control slides, omitting the primary or the secondary antibody, were run in parallel.

### Western immunoblotting

Protein lysates from ventral prostate tissue were isolated using Trizol reagent (Molecular Research Center, Inc., Cincinnati, OH). Protein concentrations were determined using the bicinchoninic acid assay (Pierce Chemical Co., Rockford, IL). Two hundred milligrams of protein were resolved on 7.5% SDS-PAGE gels and transferred to 0.2-$\mu$m supported nitrocellulose membranes (Bio-Rad Laboratories, Inc., Richmond, CA). Nonspecific binding was eliminated by preincubation in 1% heat-denatured casein for 1 h. The membranes were incubated in the appropriate dilution of the primary antibody [anti-p190 Rho-GAP, 1:500 (Transduction Laboratories, Inc.), or anti-p120 Ras-Gap, 1:1000 (Upstate Biotechnology, Inc., Lake Placid, NY)], followed by horseradish peroxidase-conjugated goat antimouse secondary antibody (1:3000; Caltag Laboratories, Inc., San Francisco, CA), developed using an enhanced chemiluminescent kit (Amersham), and exposed to X-Omat AR film (Eastman Kodak Co.) at room temperature.

## Results

To examine gene regulation during the apoptotic processes in the rat ventral prostate after hormone ablation, we performed differential display on rat ventral prostate total RNA in control animals and animals 4 days after castration. A number of sequences were present in the day 4 lane but not in the day 0 lane of the differential display (data not shown). These sequences probably represent mRNA sequences that are up-regulated during the apoptotic process. One of these sequences, designated 25.2, has 96% homology to mouse p190B at the nucleic acid level in the region homologous to a portion of the glucocorticoid receptor repression factor-1 (GRF-1)-like domain (Fig. 1). Homology to rat p190A, the second member of the p190 family, was significantly lower ($\sim$64%).

RNase protection assays using the 226-bp 25.2 complementary DNA (cDNA) fragment isolated and cloned from the differential display and total RNA extracted from the rat
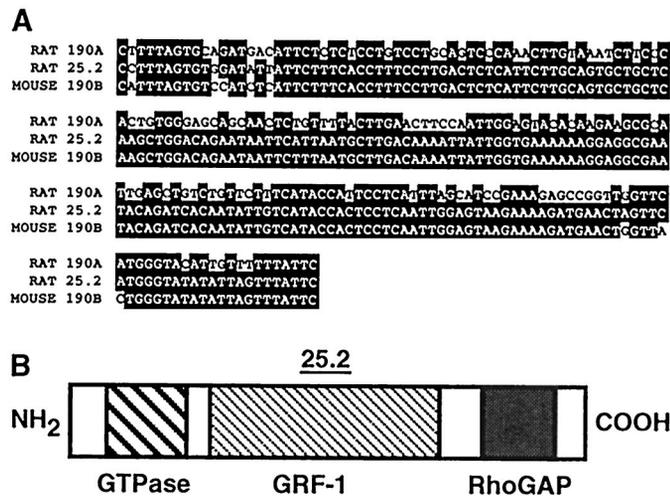
**A**



**B**



FIG. 1. Sequence homology of 25.2 and mouse p190B and rat p190A. A, 25.2 has 96% homology with mouse p190B and 64% homology with rat p190A at the nucleic acid level. B, p190A contains several domains homologous to GTPase domains: GRF-1, Rho-GAP, and GTPase-activating domain. The region of homology to 25.2 is shown *above* the domain map (adapted from Ref. 26).
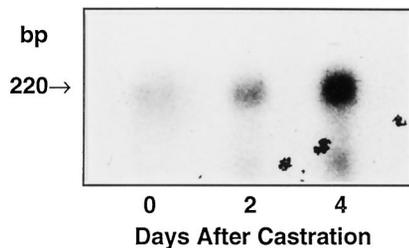


FIG. 2. RNase protection assay of 25.2. Rats were castrated, and tissues were excised on days 0, 2, and 4 after castration. RNase protection assays using the 226-bp cDNA corresponding to 25.2 were performed as described in *Materials and Methods*. The probe hybridizes to mRNA extracted from the prostate in control animals and from animals 2 and 4 days after castration and protects a 220-bp fragment.
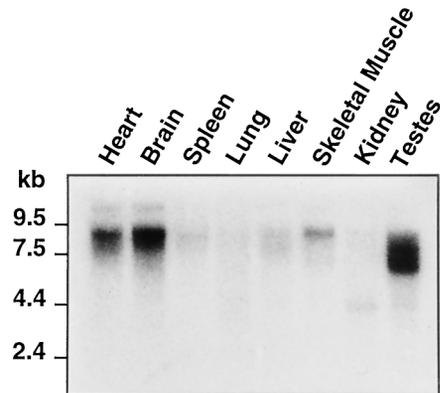


FIG. 3. Tissue distribution of cognate mRNAs hybridizing to 25.2 in the Sprague Dawley rat. A commercially available Northern blot was hybridized with radiolabeled 25.2 ($2 \times 10^6$ cpm/ml), washed, and autoradiographed as described in *Materials and Methods*. An 8.3-kb mRNA is abundantly expressed in heart, brain, skeletal muscle, and testis and is present at lower levels in spleen, lung, liver, and kidney. In addition, mRNA species of 7.6 and 6.4 kb are seen in heart, brain, and testis, and 4.4-kb mRNA is also expressed in kidney and testis.

ventral prostate on days 0, 2, and 4 after castration showed an increase in the expression of sequences protected by 25.2 on both days 2 and 4 after castration, the days on which the epithelial cells in the ventral prostate undergo apoptosis and the surviving tissue is remodeled (Fig. 2).

As neither RT-PCR nor $S_1$-nuclease analysis provides information regarding the size of the full-length mRNA, we used Northern analysis to demonstrate that 25.2 hybridizes to a RNA transcript of the appropriate size. Northern analysis using the 25.2 gene fragment on a multiple tissue blot demonstrated that 25.2 hybridizes to a mRNA of 8.3 kb. This mRNA was present at significant levels in heart, brain, skeletal muscle, and testis and at lower levels in spleen, lung, liver, and kidney (Fig. 3). The size of this mRNA corresponds to that published for p190A (26). However, the probe also hybridizes to 7.6- and 6.4-kb mRNA in heart, brain, and testis and to a 4.4-kb mRNA in kidney and testis. The 6.4-kb band probably corresponds to p190B mRNA (24), suggesting that the 25.2 cDNA hybridizes to both p190A and p190B. The identities of the 7.6- and 4.4-kb mRNAs and their relationship to the p190 family have not been further investigated.

RT-PCR analysis demonstrated that the steady state level of p190A mRNA increased in the rat ventral prostate after hormone ablation when standardized against GAPDH levels (Fig. 4A). In the same samples, the steady state level of p190B mRNA remained relatively constant throughout the time course (Fig. 4B).

Western analysis demonstrated that p190A was expressed in the prostate of hormone-replete animals and that the steady state level of the p190A protein increased approximately 20-fold in the ventral prostate during regression (Fig. 5A). In contrast, the modest 2-fold increase in the steady state level of p120 RasGAP was probably not significant (Fig. 5B). Regardless of whether the increase in p120 RasGAP was significant, it is clear that the relative level of p190 to p120 RasGAP increased between 10- and 20-fold. Immunohistochemical analysis showed that the p190A protein was expressed in normal prostatic tissue, primarily in the tall columnar epithelial cells (Fig. 6A). During regression, levels of the protein increased in the tall columnar epithelial cells. Higher magnification suggests that the localization of the protein also changed. In the ventral prostate of intact rats, the protein appeared to be diffusely localized throughout the cytoplasm (Fig. 6A, *inset*). After castration, the level of cytoplasmic staining clearly increased by day 2, and by day 4 after castration, the protein appeared to be more predominantly localized to the lumenal aspect of the cell, particularly in the perinuclear region, possibly associated with cytoskeletal processes (Fig. 6C, *inset*). There was also a significant increase in the immunofluorescence in the stromal compartment starting on day 2 after castration (Fig. 6B). By day 4 after castration, most of the cells in the stroma appeared to express significant levels of p190A (Fig. 6C).

## Discussion

Using differential display RT-PCR we have identified a sequence that is up-regulated in the rat ventral prostate after castration. This sequence displays a high degree of homology to p190, a protein that has been implicated in cytoskeletal reorganization (25, 26). The data demonstrate that the levels
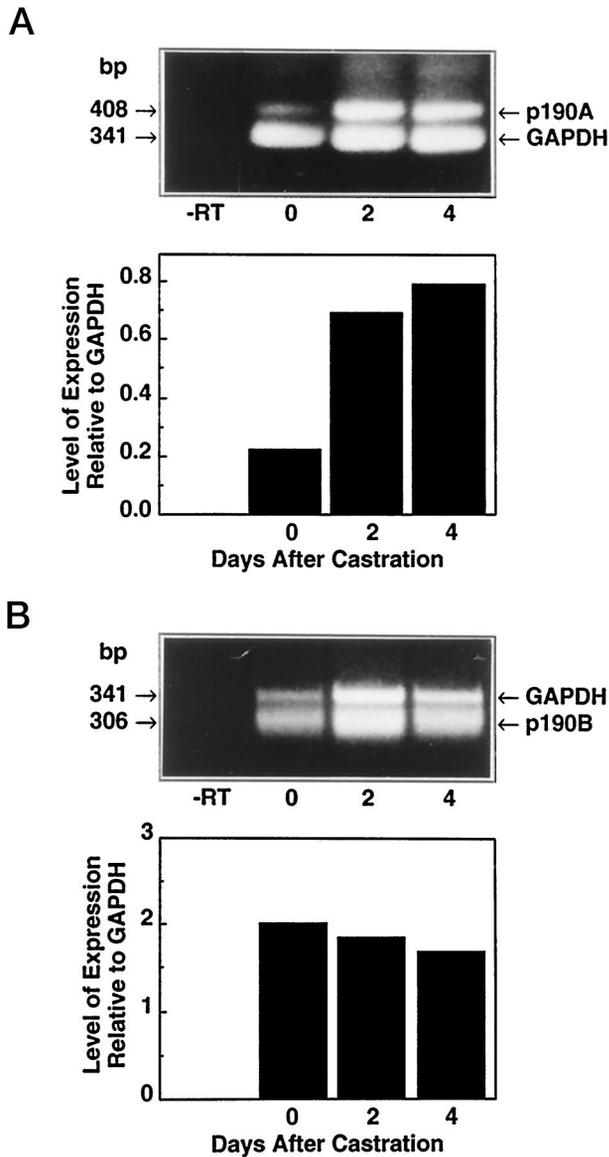
FIG. 4. Steady state levels of p190A and p190B mRNA in the rat ventral prostate after castration. RT-PCR was performed using primers specific for p190A (A) and p190B (B), using GAPDH as an internal control as described in *Materials and Methods*. mRNA extracted from the rat ventral prostate after castration was used as template. p190A and GAPDH, and p190B and GAPDH were amplified in the same reactions. p190A primers produce a band of 408 bp; p190B primers produce a band of 306 bp; GAPDH primers produce a band of 341 bp. The ratios of p190A/GAPDH and p190B/GAPDH were determined after scanning densitometry of negatives, as described in *Materials and Methods*. Representative results from one of three independent experiments are shown.
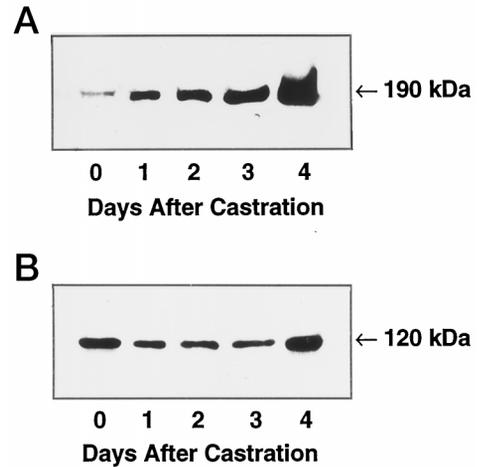


FIG. 5. Protein expression of p190A in the rat ventral prostate after castration. Western analysis of p190A (A) and p120 Ras-GAP (B) in the rat ventral prostate after castration. Protein was extracted and separated by gel electrophoresis, transferred to nitrocellulose membranes, and localized by enhanced chemiluminescence as described in *Materials and Methods*.

of both p190A mRNA and protein increase primarily in the epithelial cells of the rat ventral prostate. During the apoptotic process these cells lose their cytoskeletal structure and shape, as they become more rounded and refractile.

Two members of the p190 family have been described to date (24, 26). p190A mRNA is a ubiquitous mRNA, approximately 8.3 kb in size, which has significant sequence homology to GRF-1, a 95-kDa protein that is a transcriptional repressor of the glucocorticoid receptor gene (27). p190B appears to be encoded by a transcript of 6.4 kb, and the gene product has 51% amino acid homology to p190A (24). A second transcript of 4.4 kb hybridizes to p190A cDNA, but appears to be too small to encode the mature protein (24). As 25.2 hybridizes to the appropriate size mRNA species previously described for p190 and has significant sequence homologies to both p190A and p190B, these data suggest that 25.2 encodes one or both of the p190 isoforms. It is important to note in this context that the expression of p190 mRNA in other tissues does not necessarily correlate to the relative sensitivity to apoptosis of these tissues, as it is likely that it is the change in the level of the gene product relative to those of the other molecules required for cytoskeletal stability or the posttranslational modification of the protein that modulate the effects of p190.

The amino-terminal of p190A has sequence similarity to members of the GTPase superfamily, whereas the carboxyl-terminal shows significant homology to RhoGAP, the breakpoint cluster region gene product (24, 28), and *n*-chimerin, both of which possess intrinsic GAP activity for small GTPases (29). The amino-terminal portion of p190B contains several motifs characteristic of a GTPase domain, binds GTP and GDP (24, 28), and promotes GTP hydrolysis (28), whereas its carboxyl-terminal also contains a Rho-GAP domain (24). *In vitro* both p190 A and B have been shown to possess GAP activity and a preference for the Rho and Rac families as substrates (29, 30). p190 also interacts with p120 Ras-GAP (24). SH$_2$-phosphotyrosine interactions regulate Ras-GAP-p190 association through the amino- and carboxyl-terminal SH2 domains of Ras-GAP that synergistically bind phosphorylated p190, mediating complex formation (31). The formation of a complex between Ras-GAP and p190 may couple signaling pathways that involve Ras and Rho GTPases (29, 32). It has been shown that the stimulation of Swiss 3T3 fibroblasts in culture with lysophosphatidic acid (LPA) leads to the rapid formation of stress fibers, a process dependent on Rho proteins and p125$^{FAK}$ phosphorylation
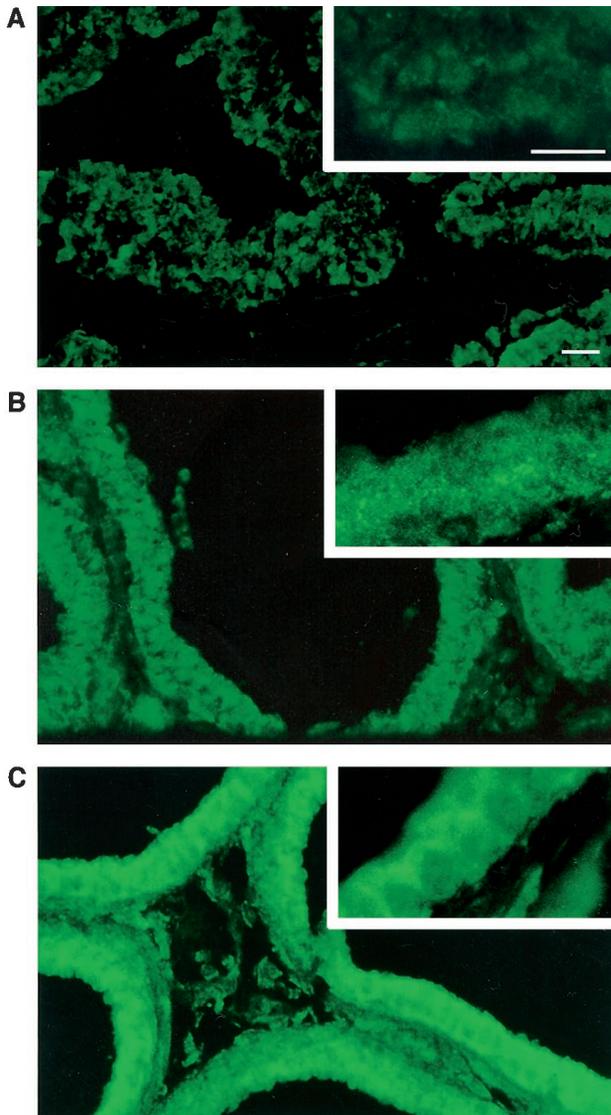
FIG. 6. Immunohistochemical localization of p190A in the ventral prostate after hormonal ablation. Rat ventral prostates were excised frozen in isopentane, sectioned at 10 mm, and stained for p190A as described in *Materials and Methods*. All sections were processed and photographed under identical conditions. A, Ventral prostrate excised from intact rats. B, Ventral prostate excised from rats castrated 2 days previously. C, Ventral prostate excised from rats castrated 4 days previously. *Bar*, 30 mm.

(30, 33–35). Furthermore, incubation with C3 exoenzyme, which inactivates Rho proteins, inhibits LPA-induced p125$^{FAK}$ phosphorylation (35). p190 inhibits LPA-stimulated stress fiber formation as a consequence of down-regulating Rho proteins that regulate the actin cytoskeleton (33, 36). Microinjection of p190 GAP into Swiss 3T3 cells causes the cells to become more rounded and refractile and to lose actin stress fibers (33, 36). This suggests a link among p190, Rho, pp125$^{FAK}$, and cell adhesion (24, 32, 35, 37).

At first glance, it might be expected that the increased levels of p190 would be preferentially localized to the membrane, rather than the perinuclear and cytoplasmic localization shown in Fig. 6. The localization of p190A to the membrane is probably dependent on several additional

factors, and the increase in perinuclear staining (as opposed to the membrane staining) may be due to the concomitant loss of membrane-associated binding partners, such as p120RasGAP or p125$^{FAK}$, to changes in their phosphorylation state, or to changes in the phosphorylation state of p190A itself. It is also possible that the increased expression of p190A results in disequilibrium in the binding stoichiometry either at the focal adhesion sites, resulting in the formation of cytoplasmic complexes that no longer maintain an active focal adhesion, or possibly with p120 Ras GAP, which might, in turn, disrupt the normal phosphorylation of p125$^{FAK}$ needed to maintain the adhesion plaque.

This implies that the induction of p190A during the apoptotic process, either complexed with p120 Ras-GAP or independently, may be involved in the dissolution of the cytoskeletal architecture of the columnar epithelial cells. Increased p190A GAP activity could lead to inactivation of the Rho GTPases, leading to the dephosphorylation of pp125$^{FAK}$, causing the cell to round up, culminating in the cytoplasmic condensation phase of apoptosis. Thus, the increase in cellular content of p190A, although clearly correlated to apoptosis in the prostate, may not be sufficient to induce apoptosis unless other protein-protein interactions are also disrupted. Whether the increased cellular content of p190A and its perinuclear relocalization can initiate the apoptosis or merely represent the later stages of the process remains to be determined. However, the induction of p190A and its effect on the cellular architecture coupled with the degradation of the extracellular proteases provide the necessary reduction in cell-substratum interactions to ensure that the dying cells are able to effectively undergo the cytoplasmic condensation that is essential for completion of apoptosis. It should be kept in mind, however, that the level of p190A expression also appears to increase in the stromal compartment, albeit to a lesser extent. It, therefore, remains possibile that the induction of p190A in both compartments may be related more to the remodeling of the tissue during regression than to the apoptotic process itself.

Finally, it should be noted that even though we have established that p190A levels in the ventral prostate increase after hormone ablation, whereas p190B levels do not change substantially, this does not preclude the possibility that the increase in the intensity of the 25.2 band detected by differential display and RNase protection is due at least in part to a third mRNA that contains the same conserved domain. We are currently exploring this possibility.

## Acknowledgments

## References

1. **Clarke PG** 1990 Developmental cell death: morphological diversity and multiple mechanisms. Anat Embryol 181:195–213
2. **Clarke PG, Clarke S** 1995 Historic apoptosis. Nature 378:230
3. **Zakeri Z, Bursch W, Tenniswood M, Lockshin R** 1995 Cell death: programmed, necrosis or other? Cell Death Differ 2:83–92
4. **Cohen JJ** 1993 Apoptosis. Immunol Today 14:126–130
5. **Zamzami N, Susin SA, Marchetti P, Hirsch T, Gomez-Monterrey I, Castedo**

M, Kroemer G 1996 Mitochondrial control of nuclear apoptosis. J Exp Med 183:1533–1544

6. Marchetti P, Castedo M, Susin SA, Zamzami N, Hirsch T, Macho A, Haeffner A, Hirsch F, Geuskens M, Kroemer G 1996 Mitochondrial permeability transition is a central coordinating event of apoptosis. J Exp Med 184:1155–1160

7. Sandford NL, Searle JW, Kerr JF 1984 Successive waves of apoptosis in the rat prostate after repeated withdrawal of testosterone stimulation. Pathol 16:406–410

8. Sensibar JA, Griswold MD, Sylvester SR, Buttyan R, Bardin CW, Cheng CY, Dudek S, Lee C 1991 Prostatic ductal system in rats: regional variation in localization of an androgen-repressed gene product, sulfated glycoprotein-2. Endocrinology 128:2091–2102

9. Sugimura Y, Cunha GR, Donjacour AA 1986 Morphological and histological study of castration-induced degeneration and androgen-induced regeneration in the mouse prostate. Biol Reprod 34:973–983

10. Rouleau M, Léger J, Tenniswood M 1990 Ductal heterogeneity of cytokeratins, gene expression, and cell death in the rat ventral prostate. Mol Endocrinol 4:2003–2013

11. English HF, Santen RJ, Isaacs JT 1987 Response of glandular versus basal rat ventral prostatic epithelial cells to androgen withdrawal and replacement. Prostate 11:229–242

12. Léger JG, Montpetit ML, Tenniswood MP 1987 Characterization and cloning of androgen-repressed mRNAs from rat ventral prostate. Biochem Biophys Res Commun 147:196–203

13. Tenniswood MP, Guenette RS, Lakins J, Mooibroek M, Wong P, Welsh JE 1992 Active cell death in hormone-dependent tissues. Cancer Metastasis Rev 11:197–220

14. Guenette RS, Mooibroek M, Wong K, Wong P, Tenniswood M 1994 Cathepsin B, a cysteine protease implicated in metastatic progression, is also expressed during regression of the rat prostate and mammary glands. Eur J Biochem 226:311–321

15. Sensibar JA, Liu XX, Patai B, Alger B, Lee C 1990 Characterization of castration-induced cell death in the rat prostate by immunohistochemical localization of cathepsin D. Prostate 16:263–276

16. Freeman SN, Rennie PS, Chao J, Lund LR, Andreasen PA 1990 Urokinase- and tissue-type plasminogen activators are suppressed by cortisol in the involuting prostate of castrated rats. Biochem J 269:189–193

17. Muntzing J 1980 Androgen and collagen as growth regulators of the rat ventral prostate. Prostate 1:71–78

18. Juliano RL, Haskill S 1993 Signal transduction from the extracellular matrix. J Cell Biol 120:577–585

19. Getzenberg RH, Pienta KJ, Coffey DS 1990 The tissue matrix: cell dynamics and hormone action. Endocr Rev 11:399–417

20. Pienta KJ, Murphy BC, Getzenberg RH, Coffey DS 1991 The effect of extracellular matrix interactions on morphologic transformation in vitro. Biochem Biophys Res Commun 179:333–339

21. Muntzing J 1988 Regulation of prostatic growth. Growth-limiting mechanisms in the rat ventral prostate. Scand J Urol Nephrol [Suppl] 107:52–55

22. Terry DE, Clark AF 1996 Glycosaminoglycans in the three lobes of the rat prostate following castration and testosterone treatment. Biochem Cell Biol 74:653–658

23. Terry DE, Clark AF 1996 Influence of testosterone on chondroitin sulphate proteoglycan in the rat prostate. Biochem Cell Biol 74:645–651

24. Burbelo PD, Miyamoto S, Utani A, Brill S, Yamada KM, Hall A, Yamada Y 1995 p190-B, a new member of the Rho Gap family, and Rho are induced to cluster after integrin cross-linking. J Biol Chem 270:30919–30926

25. Aviv H, Leder P 1972 Purification of biologically active globin messenger RNA by chromatography on oligothymidylic acid-cellulose. Proc Natl Acad Sci USA 69:1408–1412

26. Settleman J, Narasimhan V, Foster LC, Weinberg RA 1992 Molecular cloning of cDNAs encoding the GAP-associated protein p190:implications for a signaling pathway from Ras to the nucleus. Cell 69:539–549

27. LeClerc S, Palaniswami R, Xie BX, Govindan MV 1991 Molecular cloning and characterization of a factor that binds the human glucocorticoid receptor gene and represses its expression. J Biol Chem 266:17333–17340

28. Foster R, Hu KQ, Shaywitz DA, Settleman J 1994 p190 RhoGap, the major RasGap-associated protein, binds GTP directly. Mol Cell Biol 14:7173–7181

29. Settleman J, Albright CF, Foster LC, Weinberg RA 1992 Association between GTPase activators for Rho and Ras families. Nature 359:153–154

30. Ridley AJ 1994 Signal transduction through the GTP-binding proteins Rac and Rho. J Cell Sci [Suppl] 18:127–131

31. Bryant SS, Briggs S, Smithgall TE, Martin GA, McCormick F, Chang JH, Parsons SJ, Jove R 1995 Two SH2 domains of p120 Ras GTPase-activating protein bind synergistically to tyrosine phosphorylated p190 Rho GTPase-activating protein. J Biol Chem 270:17947–17952

32. McGlade J, Brunkhorst B, Anderson D, Mbamalu G, Settleman J, Dedhar S, Rozakis-Adcock M, Chen LB, Pawson T 1993 The N-terminal region of GAP regulates cytoskeletal structure and cell adhesion. EMBO J 12:3073–3081

33. Ridley AJ, Hall A 1994 Signal transduction pathways regulating Rho-mediated stress fibre formation: requirement for a tyrosine kinase. EMBO J 13:2600–2610

34. Ridley AJ, Paterson HF, Johnston CL, Diekmann D, Hall A 1992 The small GTP-binding protein rac regulates growth factor-induced membrane ruffling. Cell 70:401–410

35. Kumagai N, Morii N, Fujisawa K, Nemoto Y, Narumiya S 1993 ADP-ribosylation of rho p21 inhibits lysophosphatidic acid-induced protein tyrosine phosphorylation and phosphatidylinositol 3-kinase activation in cultured Swiss 3T3 cells. J Biol Chem 268:24535–24538

36. Ridley AJ, Self AJ, Kasmi F, Paterson HF, Hall A, Marshall CJ, Ellis C 1993 Rho family GTPase activating proteins p190, Bcr and RhoGap show distinct specificities in vitro and in vivo. EMBO J 12:5151–5160

37. Ridley AJ, Hall A 1992 The small GTP-binding protein rho regulates the assembly of focal adhesions and actin stress fibers in response to growth factors. Cell 70:389–399